SAR Benefits of Including E-field Interactions in Parallel RF Pulse Design

C. M. Deniz[1,2], L. Alon[1,2], R. Lattanzi[1,2], D. K. Sodickson[1], and Y. Zhu[1]

[1]Center for Biomedical Imaging, Department of Radiology, NYU School of Medicine, New York, NY, United States, [2]Sackler Institute of Graduate Biomedical Sciences, NYU School of Medicine, New York, NY, United States

Introduction

Electric field (E-field) interactions inside the object must be taken into account for specific absorption rate (SAR) management in parallel transmission systems [1]. At a recent conference, Zhu [2] introduced a new method to measure the E-field covariance matrix, **Φ,** in a rapid and subject-specific manner. RF pulse design that incorporates knowledge of **Φ** can result in reduced SAR with preserved excitation fidelity [3]. In this work we investigate the global SAR benefits of employing **Φ** for RF pulse design optimization, simulating various experimental setups with different **Φ** characteristics. The effectiveness of incorporating the **Φ**-matrix into RF pulse design was then evaluated and the results showed improved SAR management over current optimization practices.

Methods

A 4-element transmit array was simulated using the Finite Difference Time Domain method (xFDTD 6.3, REMCOM, State College, PA) in a 7T environment, using both a homogenous rectangular water phantom (conductivity 0.6 SI/m) and a human mesh dataset (5x5x5mm^3 voxel size). E-fields and B_1^+ fields of each transmit element were calculated by driving the coil of interest with a unit current, while keeping the other coils dormant.

The target excitation profile $\mathbf{m}_{des}$ were 10° and 90° flip angle distributions on a uniform coronal disk with diameter equal to 15 cm at the center of FOV for small-tip-angle (STA) and large-tip-angle (LTA) design, respectively. Inward spiral trajectory was used to cover the excitation k-space, using the following parameters: number of spiral turns=12, sampling interval=10μs and duration= 5 ms, resolution=10mm, gradient slew rate=150mT/m/s, gradient amplitude=40mT/m. Acceleration was achieved undersampling the *k*-space trajectory radially.

We used the small tip angle method [4] to design STA excitation pulses by solving $\underset{\mathbf{b}_{full}}{\arg\min}\left\{\left\|\mathbf{A}_{full}\mathbf{b}_{full}-\mathbf{m}_{des}\right\|_{\mathbf{w}}^{2}+R\left(\mathbf{b}_{full}\right)\right\}$ where $\mathbf{b}_{full}$ is the RF pulse waveform of all coils, and $\mathbf{A}_{full}$ is the system matrix. The 90° excitation pulse was designed using the linear class LTA method [5], by solving $\underset{\mathbf{b}_{full}}{\arg\min}\left\{\left\|\mathbf{S}_{full}\mathbf{b}_{full}-\boldsymbol{\theta}_{des}\right\|_{\mathbf{w}}^{2}+R\left(\mathbf{b}_{full}\right)\right\}$ where $\boldsymbol{\theta}_{des}$ is the target flip angle distribution and $\mathbf{S}_{full}$ is the system matrix. Two different regularization terms were introduced into the design scheme: $R\left(\mathbf{b}_{full}\right)=\beta\mathbf{b}_{full}^{H}\mathbf{I}\mathbf{b}_{full}$ to penalize only integrated RF current and $R\left(\mathbf{b}_{full}\right)=\beta\mathbf{b}_{full}^{H}\boldsymbol{\Phi}\mathbf{b}_{full}$ to penalize global SAR, where β is the regularization parameter and **I** is the identity matrix. Calculated RF pulses were fed into a Bloch equation simulator [6] using spatial grid of 5mm to obtain the resulting magnetization profiles.

As a measure of the fidelity of the excitation, we used the normalized root-mean-square error (NRMSE) between the desired magnetization and the magnetization profile of the calculated RF pulses. NRMSE was calculated using: $NRMSE=\left\|\boldsymbol{m}_{des}-Bloch(\boldsymbol{b}_{full})\right\|_{2}/\|\boldsymbol{m}_{des}\|_{2}$. Power deposition (watts) at location *r* was calculated as: $Power(r)\cong\frac{\sigma(r)}{2T}\sum_{p=0}^{N_t-1}\|E(r,p\Delta t)\|_2^2\,\Delta t$ where σ is the electrical conductivity, T is the duration of RF pulse and $E(r,p\Delta t)=\sum_{n=1}^{N}b_n(p\Delta t)E_n(r)$, is the superposition of the electric fields of the *N* (*N*=4 in this study) multiplied by the driving RF waveforms $\mathbf{b_n}$ at each time instant *pΔt*. Global SAR was calculated as the average power over the object volume divided by the object mass.

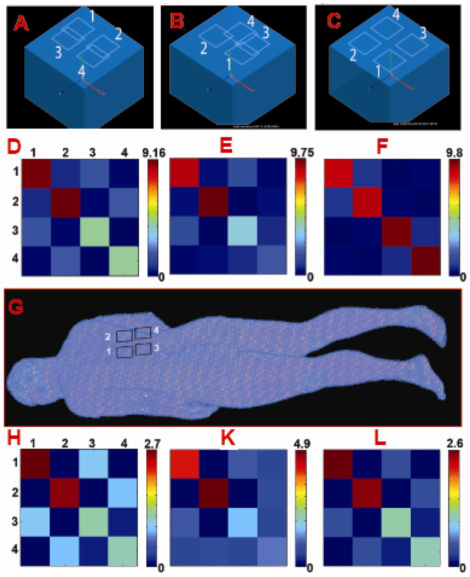

Figure 1 Experimental setup. A, B and C are different coil configurations with Φ-matrices D, E and F, respectively. G shows the location of the coils in the simulation using realistic human mesh. H, K and L are the Φ-matrices in the human mesh of the coil setups A, B and C, respectively.

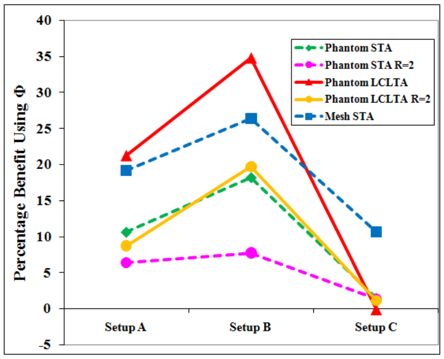

Figure 2 Variations in global SAR when the **Φ**-matrix is incorporated into parallel RF pulse design. Values are reported as the percentage of improvement with respect to using Identity matrix instead of **Φ**

In order to investigate how the effect on global SAR of including **Φ** into the parallel transmission RF pulse design varies with the structure of the E-field covariance matrix, we used three experimental setups with the four surface coils arranged in different geometrical configurations, resulting in different E-field interactions (Figure 1). Simulations were performed for unaccelerated and 2-fold (*R*=2) accelerated parallel excitations.

Results

NRMSE was kept constant using different regularization parameters between RF designs including **Φ** and **I**. Both linear class LTA and STA pulse design resulted in lower global SAR when E-field interactions were accounted for than when they were not accounted for in the design process (Figure 2). Greater SAR benefits were observed for setup B, which resulted in the largest variation between the elements of the Φ-matrix. For setup C, global SAR differences were minor in the case of the water phantom which can be explained by resemblance of the array elements to identity matrix, whereas they were about 10% in the case of human mesh. For the human mesh dataset, larger benefits were observed than for the water phantom for STA RF pulse design.

Table 1 shows that incorporating the **Φ**-matrix in RF pulse calculations results in lower global SAR for every coil without trading off excitation fidelity. SAR decrease was more significant for the arrays in setup A and B, for which stronger E-field interactions resulted in large variations among the diagonal and off-diagonals elements of the **Φ**-matrix. Although the use of the **Φ**-matrix in pulse design increased the sum of the RF current amplitudes in all channels for most of the experiments, as indicated by the values in the third row of the Table 1, that did not result in higher global SAR.

Table 1 Comparison of different setups with different acceleration factors in water phantom with STA RF pulse design

	Setup A				Setup B				Setup C			
	Acceleration =1		Acceleration =2		Acceleration =1		Acceleration =2		Acceleration =1		Acceleration =2	
	Φ	**I**	**Φ**	**I**	**Φ**	**I**	**Φ**	**I**	**Φ**	**I**	**Φ**	**I**
SAR (W/kg)	0.097	0.109	0.619	0.661	0.100	0.123	0.667	0.723	0.115	0.116	0.854	0.866
NRMSE	0.021	0.021	0.020	0.020	0.020	0.020	0.020	0.020	0.022	0.022	0.021	0.021
Total RF (A)	1283.9	1147.7	1727.0	1603.1	1555.9	1291.6	2139.9	1815.6	1053.3	1042.6	1606.6	1607.4
% SAR decrease	10.7		6.4		18.2		7.8		1.4		1.3	

Conclusions

In this work, using simulations of particular experimental conditions, we showed that there are SAR benefits in including measured E-field interactions into RF pulse design for parallel transmission. Our results suggest that knowledge of the **Φ**-matrix, which has recently been shown to be experimentally accessible, can be exploited to improve SAR management, while maintaining excitation homogeneity.

References: [1] Zhu, Y. (2004) MRM 51: 775-84. [2] Zhu, Y. ISMRM 2009, 2585. [3] Lattanzi, R, et al. (2009) MRM 616: 315-334. [4] Grissom, W, et al.(2006) MRM 56: 620-9. [5] Xu, D, et al.(2007) MRM 58: 326-34. [6] Pauly, J, et al. (1991) IEEE TMI 10: 53-65.